

# C1.2 Flow over a NACA0012 Airfoil

Lei Shi and Z.J. Wang

University of Kansas

## I. Code Description

HpMusic (HP adaptive MUltiphysics SIMulation Code) is a parallel adaptive high-order correction procedure via reconstruction (CPR) solver. It can support up to 6<sup>th</sup> order CPR schemes on hybrid QUAD/TRI meshes in 2D and HEX meshes in 3D. The code is parallelized using domain partitioning and MPI message passing library. An adjoint-based HP-adaptation is available to control the discretization error and efficiently predict the engineering output.

## II. Case Summary

All simulations start from the free stream in this case. A GMRES solver with a LU-SGS as a preconditioner is used for the time integration. The  $L_2$  norm of the density residual is used to monitor the convergence. The initial residual converged by 10 orders of magnitude for all cases in this test. The simulations were performed in the serial mode. TauBench ran in 9.65s. The “truth” outputs are obtained using adjoint-based h-adaptation with a  $p = 3$  CPR scheme. The CPU time is expressed in work units, which includes the time taken for the primal solve, the adjoint solve and the error estimation.

## III. Meshes

The second level of the quadrilateral mesh provided by the workshop website is used as the initial mesh for the adaptive simulation. Mesh refinement is performed in the original element’s polynomial space using the reference coordinates. For elements on the geometry boundaries, an extra remapping process is employed to snap the boundary points to the truth geometry during each adaptation level.

## IV. Results

### IV.A. Subsonic Inviscid Case

#### IV.A.1. Truth Output

The “truth” outputs are obtained using adjoint-based h-adaptation. We use the 4<sup>th</sup> order CPR scheme with the Gauss points as the solution points and the flux points. The DG correction function and the LP approach is used for all runs. The newly inserted grid points on every adaptation stage are remapped to the real NACA0012 airfoil to reduce the geometry approximation error. The initial mesh is refl grid from the workshop website, which consists of 560  $p4$  curved elements.

For the inviscid case, the initial mesh and the final adapted meshes using the lift and drag adjoint are shown in Figure IV.1. The convergence histories of the lift and drag coefficients are shown in Figure IV.3. The corrected outputs are computed using the adjoint-based error estimates. The results show that the corrected coefficients converge much faster than the uncorrected ones, and all converge to the same value. The estimated  $C_L$  and  $C_D$  error using the lift and drag adjoint are shown in Figure IV.2. On the final adaptation stage, the estimated output error is around  $10^{-9}$ , which has around  $3.8e^5$  and  $4.4e^5$  number of degrees of freedom for drag and lift coefficients respectively. The truth  $C_L$  and  $C_D$  are chosen from the final adaptation stage as

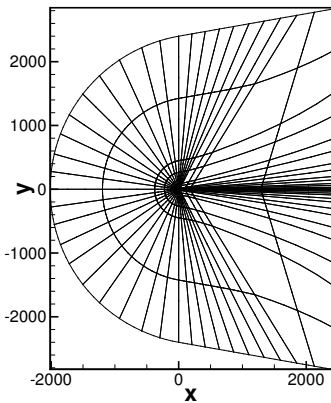
$$C_L = 0.286479458 \pm 1e^{-9}$$

$$C_D = 2.1023e^{-6} \pm 5e^{-10}$$

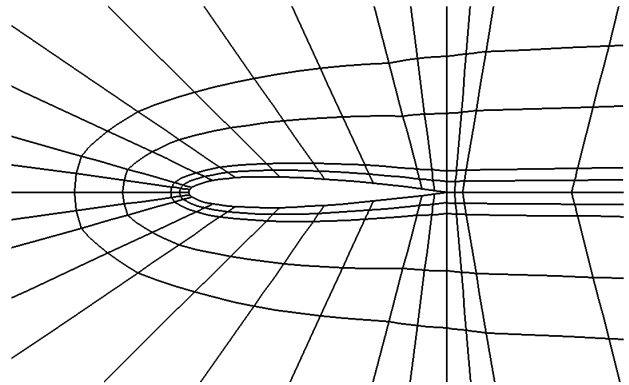
For the viscous case, the BR2 method is used to discretize the viscous term. The convergence histories of the lift and drag coefficients are shown in Figure IV.6. The estimated  $C_L$  and  $C_D$  error using the lift and drag adjoint are shown in Figure IV.5. On the final adaptation stage, the estimated output error is around  $10^{-9}$ , which has around  $2e^5$  and  $6e^5$  number of degrees of freedom for drag and lift coefficients respectively. The final adapted meshes using the lift and drag adjoint are shown in Figure IV.4. The truth  $C_L$  and  $C_D$  are chosen from the final adaptation stage as

$$C_L = 1.827337e^{-2} \pm 3e^{-8}$$

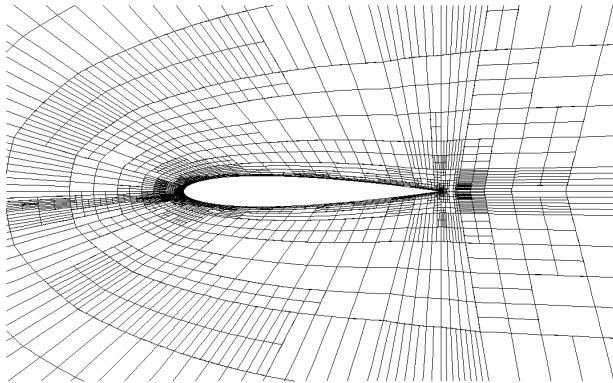
$$C_D = 5.531689e^{-2} \pm 3e^{-9}$$



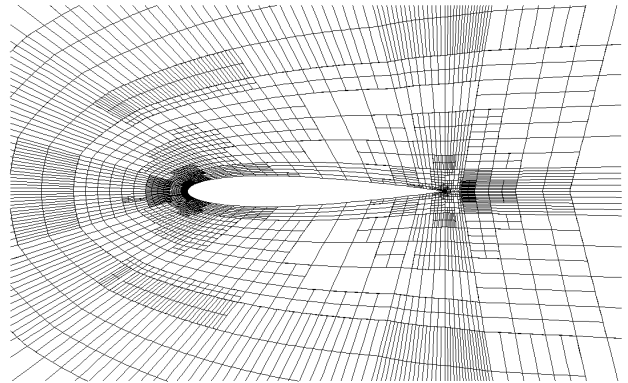
(a) The initial  $p_4$  mesh



(b) The initial  $p_4$  mesh, zoom in



(c)  $C_L$  Adjoint



(d)  $C_D$  Adjoint

Figure IV.1: Adapted mesh for the adjoint-based h-adaptation for an inviscid NACA 0012 airfoil at  $M_0 = 0.5$ ,  $\alpha = 2^\circ$  ( $p = 3$ ).

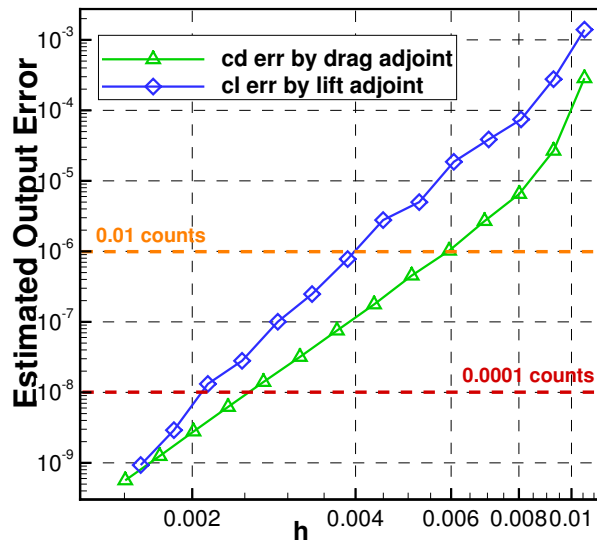


Figure IV.2: Estimated output using the adjoint-based h-adaptation for a inviscid NACA 0012 airfoil at  $M_0 = 0.5$ ,  $\alpha = 2^\circ$  ( $p = 3$ ).

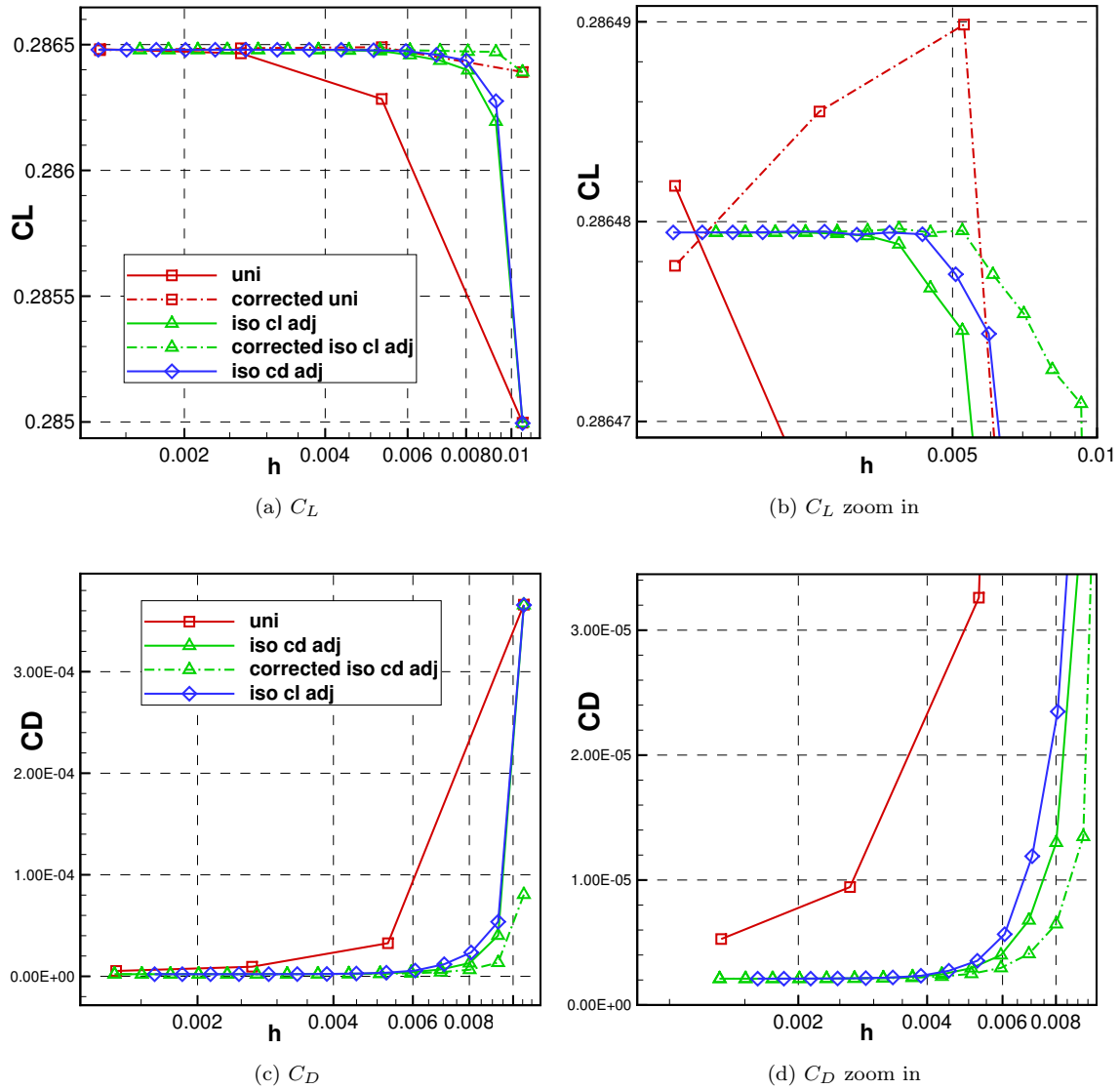


Figure IV.3:  $C_L$  and  $C_D$  convergence of the adjoint-based h-adaptation for a NACA 0012 airfoil at  $M_0 = 0.5$ ,  $\alpha = 2^\circ$  ( $p = 3$ ).

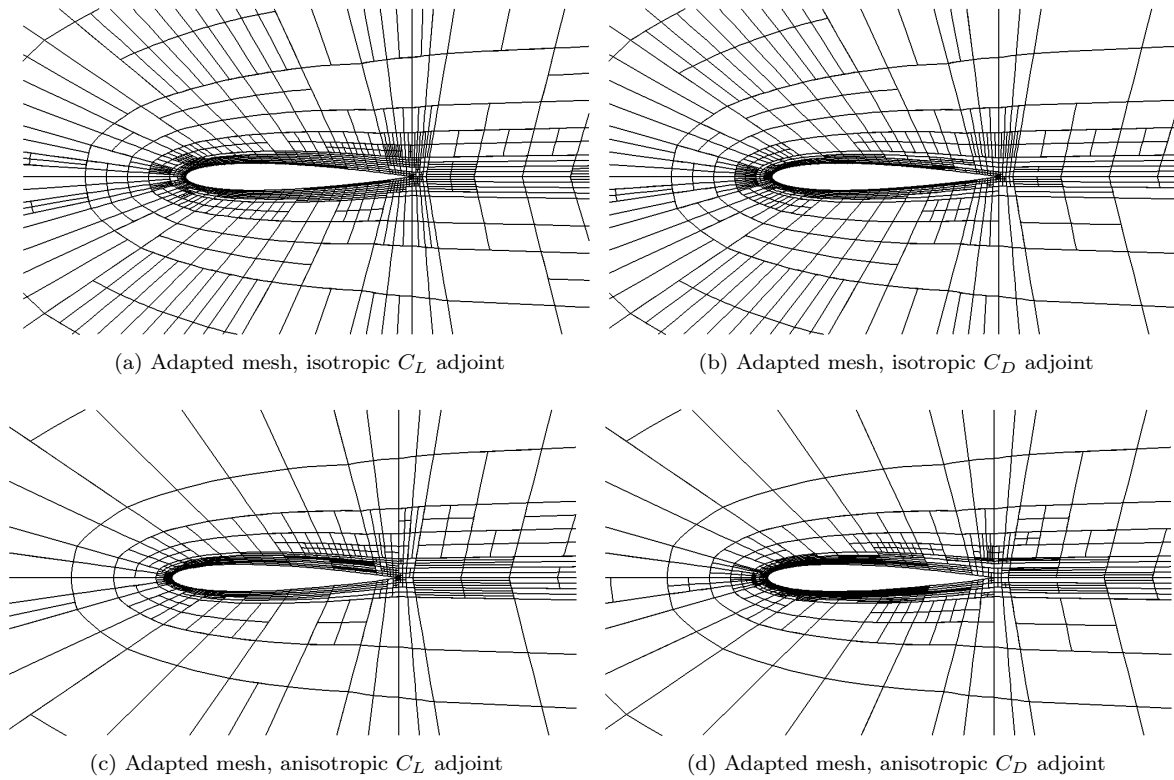


Figure IV.4: Adjoint-based h-adapted mesh for a NACA 0012 airfoil at  $M_0 = 0.5$ ,  $\alpha = 1^\circ$ ,  $Re = 5000$  ( $p = 3$ ).

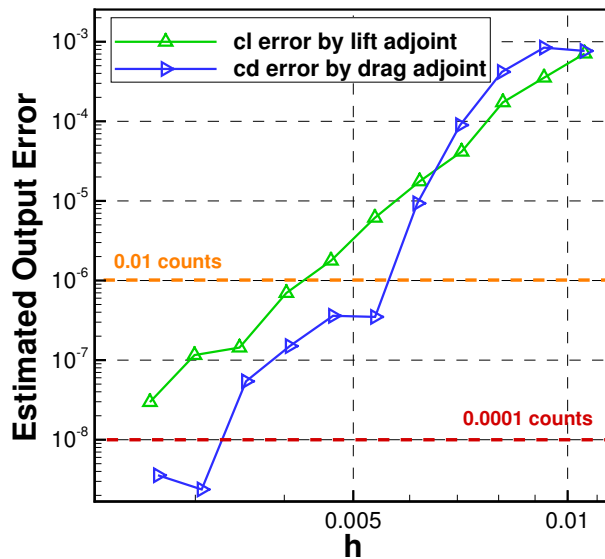
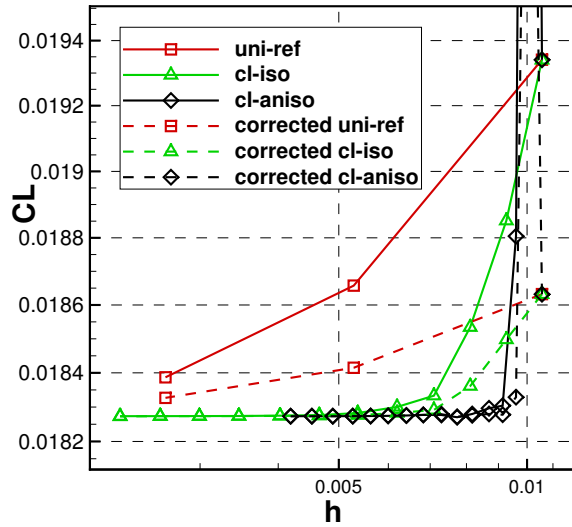
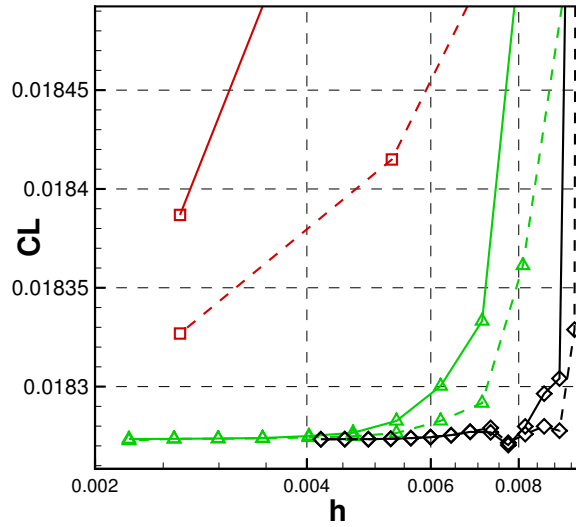


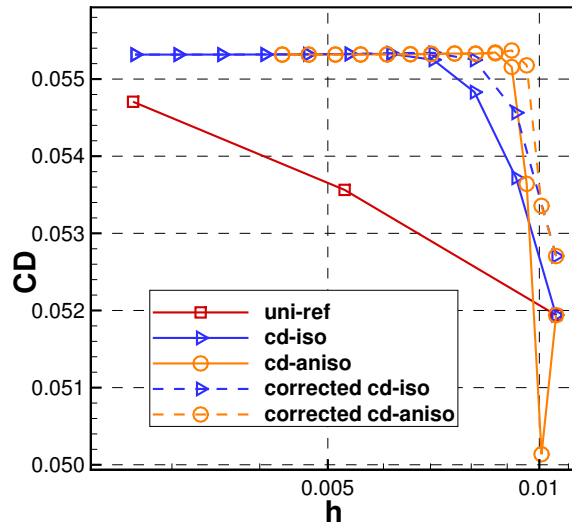
Figure IV.5: Estimated output using the adjoint-based h-adaptation for a NACA 0012 airfoil at  $M_0 = 0.5$ ,  $\alpha = 1^\circ$ ,  $Re = 5000$  ( $p = 3$ ).



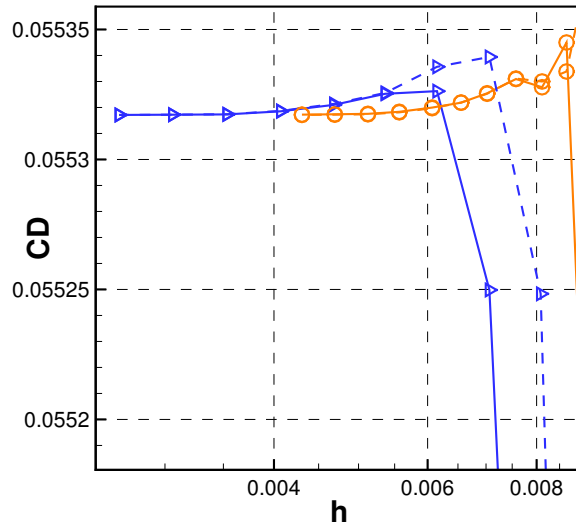
(a) CL



(b) Zoom in, CL



(c) CD



(d) Zoom in, CD

Figure IV.6: CL and CD convergence for a NACA 0012 airfoil at  $M_0 = 0.5$ ,  $\alpha = 1^\circ$ ,  $Re = 5000$  ( $p = 3$ ).

IV.A.2. Inviscid Case Results

Below figures and tables show the requested results for the inviscid flow over a NACA0012 airfoil. Discrete adjoint-based isotropic adaptations are driven by the output-based error indicator. Uniform h-refinement is performed to compare those adaptation strategies. The CPR method with the Gauss points as the SPs/FPs and the LP approach is used in the discretization. All adaptations start from the ref1 quadrilateral mesh provided by the workshop website, which has 560  $p_4$  quadrilateral elements.

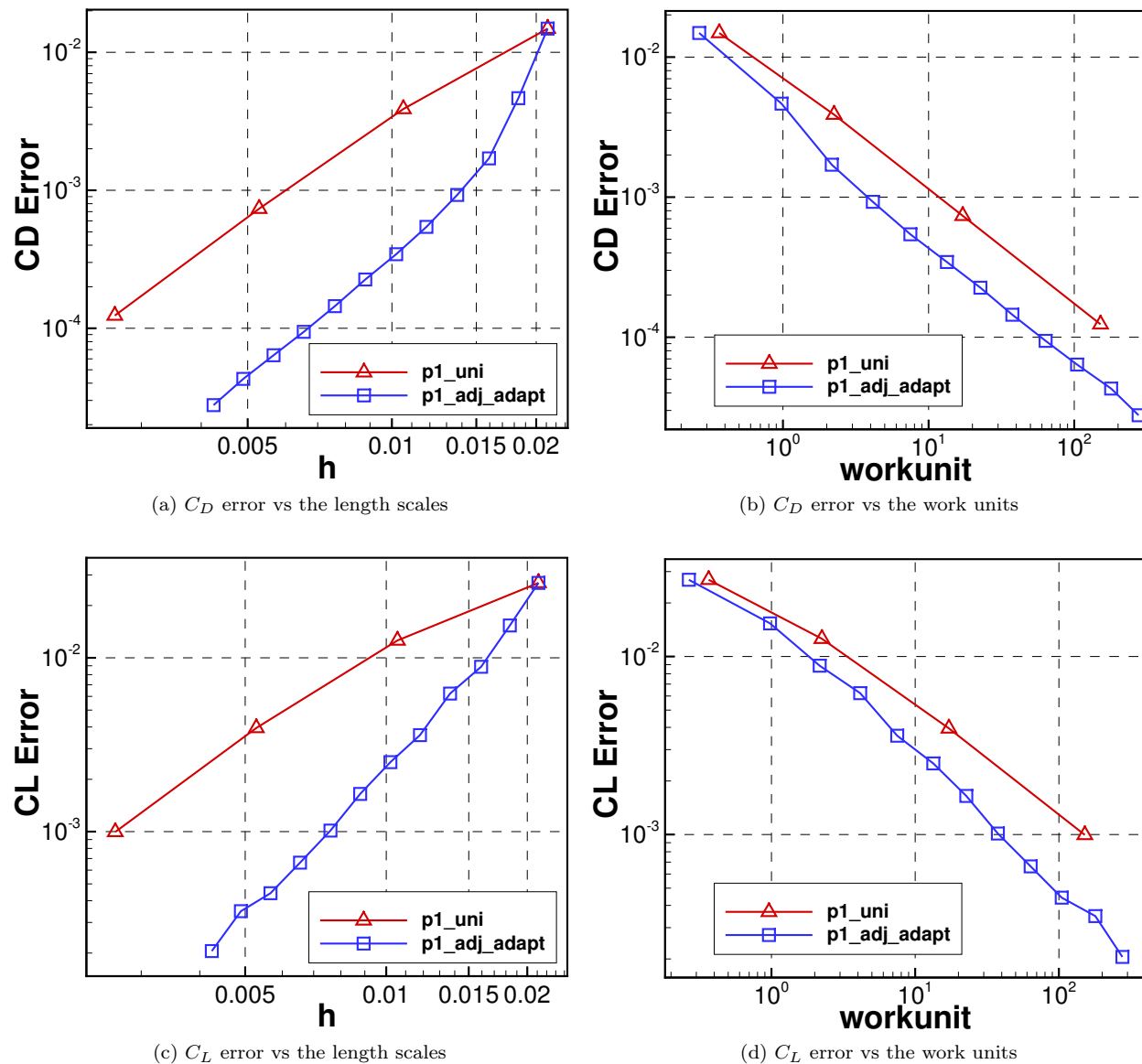
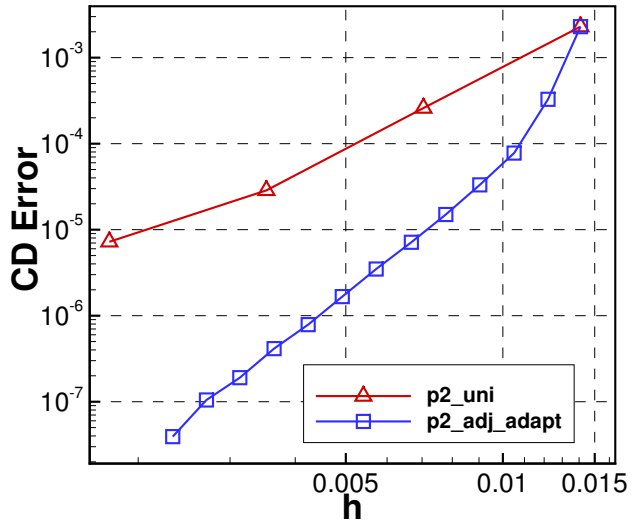
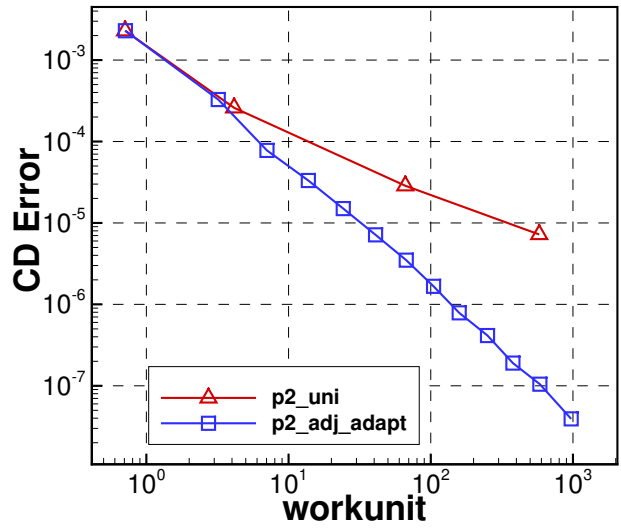


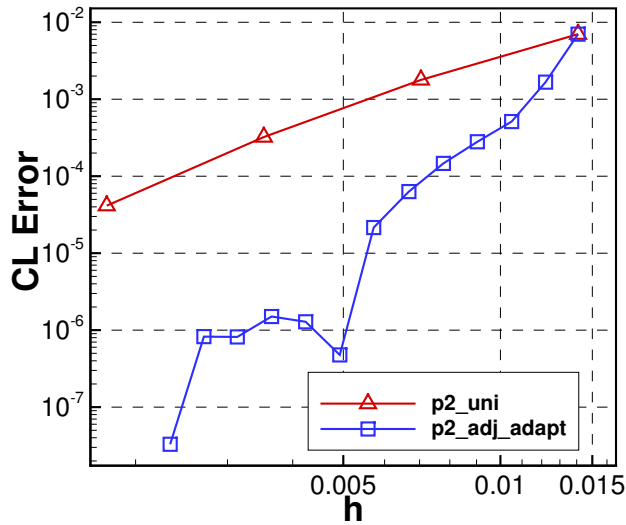
Figure IV.7: NACA 0012 airfoil at  $M_0 = 0.5$ ,  $\alpha = 2^\circ$  ( $p = 1$ ).



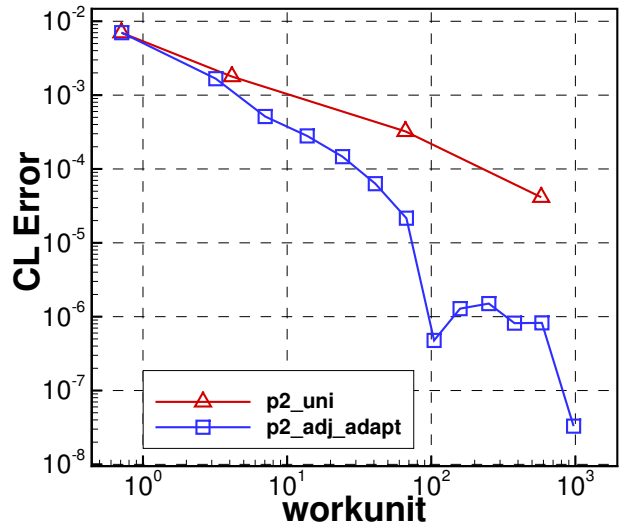
(a)  $C_D$  error vs the length scales



(b)  $C_D$  error vs the work units



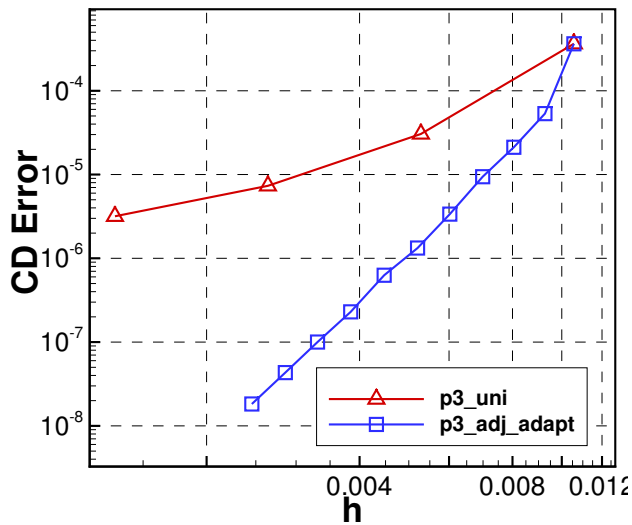
(c)  $C_L$  error vs the length scales



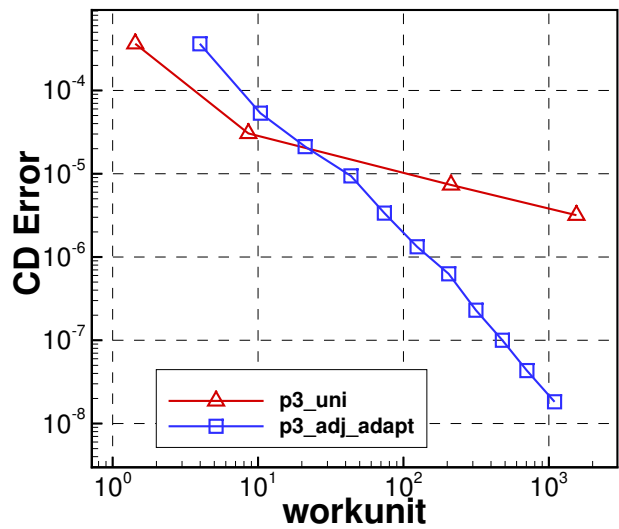
(d)  $C_L$  error vs the work units

Figure IV.8: NACA 0012 airfoil at  $M_0 = 0.5$ ,  $\alpha = 2^\circ$  ( $p = 2$ ).

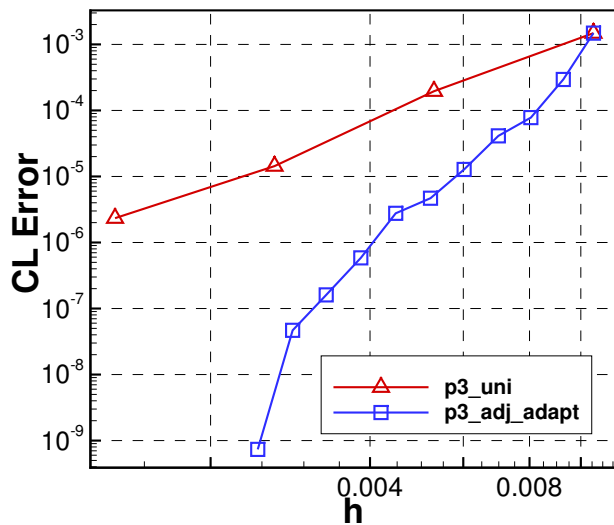




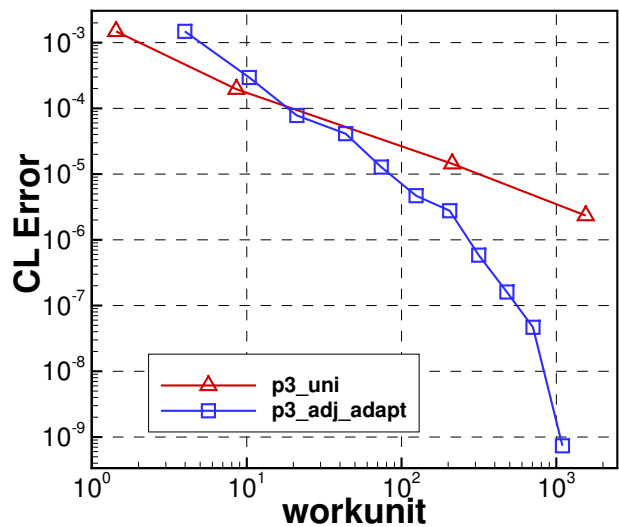
(a)  $C_D$  error vs the length scales



(b)  $C_D$  error vs the work units

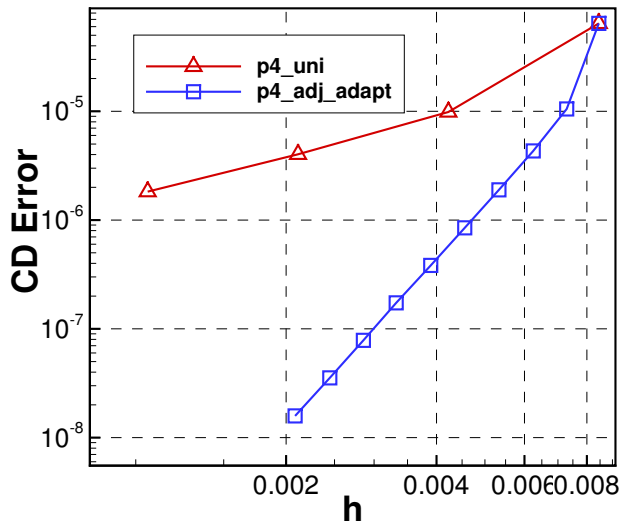


(c)  $C_L$  error vs the length scales

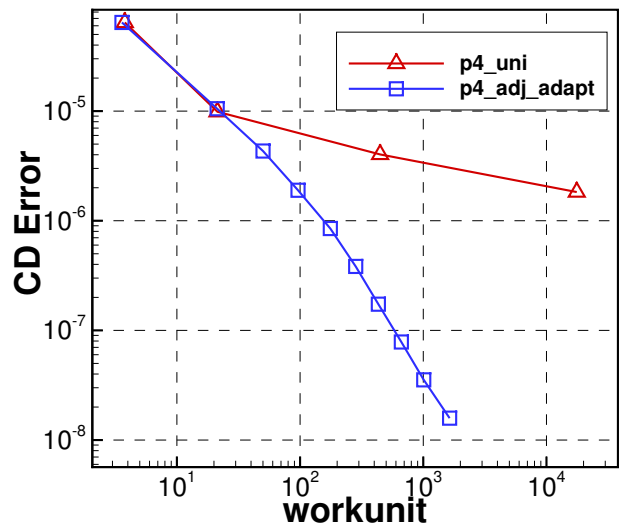


(d)  $C_L$  error vs the work units

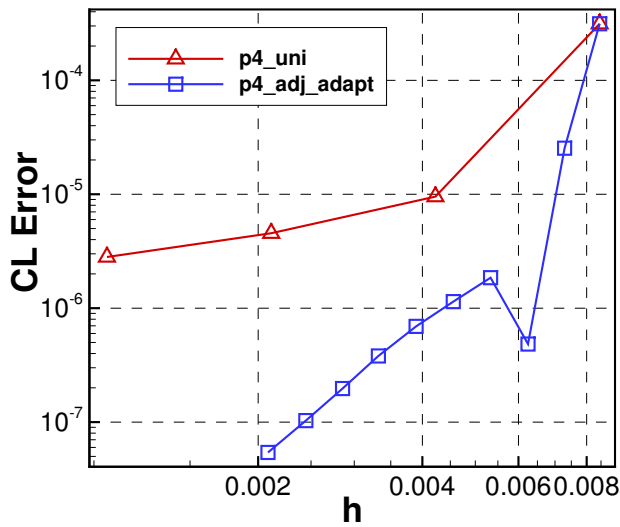
Figure IV.9: NACA 0012 airfoil at  $M_0 = 0.5$ ,  $\alpha = 2^\circ$  ( $p = 3$ ).



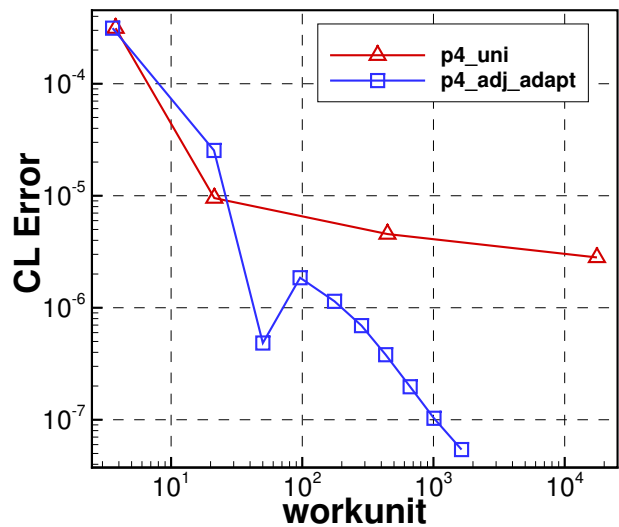
(a)  $C_D$  error vs the length scales



(b)  $C_D$  error vs the work units



(c)  $C_L$  error vs the length scales



(d)  $C_L$  error vs the work units

Figure IV.10: NACA 0012 airfoil at  $M_0 = 0.5$ ,  $\alpha = 2^\circ$  ( $p = 4$ ).

Table 1: NACA 0012 airfoil at  $M_0 = 0.5$ ,  $\alpha = 2^\circ$  ( $p = 1$ ).

adaptation stages	cell	h	$C_L$	$C_D$	$C_L$ error	$C_D$ error	work units
1	560	2.113E-02	2.594967E-01	1.485331E-02	2.70E-02	1.49E-02	2.6621E-01
2	742	1.836E-02	2.711257E-01	4.651894E-03	1.54E-02	4.65E-03	9.7783E-01
3	984	1.594E-02	2.775999E-01	1.705732E-03	8.88E-03	1.70E-03	2.1649E+00
4	1,335	1.368E-02	2.802530E-01	9.276097E-04	6.23E-03	9.26E-04	4.1434E+00
5	1,795	1.180E-02	2.828897E-01	5.448523E-04	3.59E-03	5.43E-04	7.4995E+00
6	2,400	1.021E-02	2.839702E-01	3.462358E-04	2.51E-03	3.44E-04	1.3362E+01
7	3,230	8.798E-03	2.848323E-01	2.277584E-04	1.65E-03	2.26E-04	2.2685E+01
8	4,326	7.602E-03	2.854661E-01	1.467259E-04	1.01E-03	1.45E-04	3.7601E+01
9	5,833	6.547E-03	2.858171E-01	9.629098E-05	6.62E-04	9.42E-05	6.3601E+01
10	7,797	5.662E-03	2.860375E-01	6.585701E-05	4.42E-04	6.38E-05	1.0462E+02
11	10,428	4.896E-03	2.861312E-01	4.507717E-05	3.48E-04	4.30E-05	1.7920E+02
12	13,881	4.244E-03	2.862741E-01	2.983348E-05	2.05E-04	2.77E-05	2.7657E+02

Table 2: NACA 0012 airfoil at  $M_0 = 0.5$ ,  $\alpha = 2^\circ$  ( $p = 2$ ).

adaptation stages	cell	h	$C_L$	$C_D$	$C_L$ error	$C_D$ error	work units
1	560	1.409E-02	2.794724E-01	2.292937E-03	7.01E-03	2.29E-03	7.1162E-01
2	746	1.220E-02	2.848121E-01	3.298774E-04	1.67E-03	3.28E-04	3.2007E+00
3	1,006	1.051E-02	2.859664E-01	7.986870E-05	5.13E-04	7.78E-05	7.0437E+00
4	1,362	9.032E-03	2.861992E-01	3.527380E-05	2.80E-04	3.32E-05	1.3777E+01
5	1,838	7.775E-03	2.863328E-01	1.711350E-05	1.47E-04	1.50E-05	2.4239E+01
6	2,492	6.677E-03	2.864163E-01	9.241150E-06	6.32E-05	7.14E-06	4.0916E+01
7	3,399	5.717E-03	2.864579E-01	5.591227E-06	2.15E-05	3.49E-06	6.7226E+01
8	4,585	4.923E-03	2.864799E-01	3.769123E-06	4.76E-07	1.67E-06	1.0462E+02
9	6,196	4.235E-03	2.864807E-01	2.889518E-06	1.28E-06	7.87E-07	1.5848E+02
10	8,372	3.643E-03	2.864810E-01	2.516502E-06	1.50E-06	4.14E-07	2.5067E+02
11	11,326	3.132E-03	2.864803E-01	2.292447E-06	8.17E-07	1.90E-07	3.7808E+02
12	15,207	2.703E-03	2.864803E-01	2.206981E-06	8.24E-07	1.05E-07	5.8525E+02
13	20,480	2.329E-03	2.864795E-01	2.141554E-06	3.29E-08	3.93E-08	9.7162E+02

Table 3: NACA 0012 airfoil at  $M_0 = 0.5$ ,  $\alpha = 2^\circ$  ( $p = 3$ ).

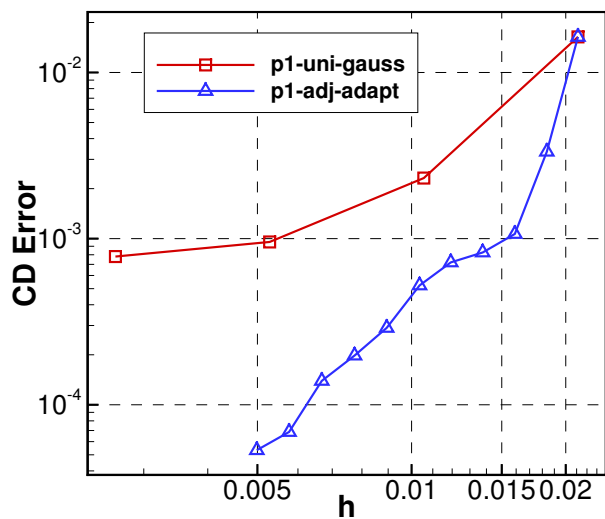
adaptation stages	cell	h	$C_L$	$C_D$	$C_L$ error	$C_D$ error	work units
1	560	1.056E-02	2.8499530E-01	3.656546E-04	1.48E-03	3.64E-04	3.9786E+00
2	728	9.266E-03	2.8618474E-01	5.544746E-05	2.95E-04	5.33E-05	1.0376E+01
3	965	8.048E-03	2.8640151E-01	2.327108E-05	7.79E-05	2.12E-05	2.1077E+01
4	1,280	6.988E-03	2.8643826E-01	1.151603E-05	4.12E-05	9.41E-06	4.3510E+01
5	1,724	6.021E-03	2.8646667E-01	5.470242E-06	1.28E-05	3.37E-06	7.3919E+01
6	2,309	5.203E-03	2.8647476E-01	3.428753E-06	4.69E-06	1.33E-06	1.2416E+02
7	3,125	4.472E-03	2.8647669E-01	2.730293E-06	2.77E-06	6.28E-07	2.0467E+02
8	4,232	3.843E-03	2.8647887E-01	2.332021E-06	5.85E-07	2.30E-07	3.1507E+02
9	5,717	3.306E-03	2.8647929E-01	2.202419E-06	1.61E-07	1.00E-07	4.7897E+02
10	7,655	2.857E-03	2.8647941E-01	2.145557E-06	4.67E-08	4.33E-08	7.0628E+02
11	10,367	2.455E-03	2.8647945E-01	2.120544E-06	7.36E-10	1.82E-08	1.0947E+03

Table 4: NACA 0012 airfoil at  $M_0 = 0.5$ ,  $\alpha = 2^\circ$  ( $p = 4$ ).

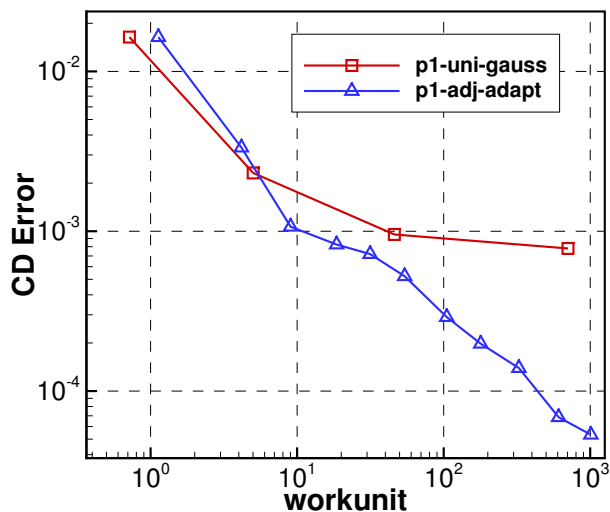
adaptation stages	cell	h	$C_L$	$C_D$	$C_L$ error	$C_D$ error	work units
1	560	8.452E-03	2.8616592E-01	6.640619E-05	3.14E-04	6.43E-05	3.5840E+00
2	753	7.288E-03	2.8645409E-01	1.261503E-05	2.54E-05	1.05E-05	2.1235E+01
3	1,025	6.247E-03	2.8647897E-01	6.424023E-06	4.84E-07	4.32E-06	5.0031E+01
4	1,406	5.334E-03	2.8648131E-01	3.998304E-06	1.85E-06	1.90E-06	9.6230E+01
5	1,927	4.556E-03	2.8648059E-01	2.951111E-06	1.14E-06	8.49E-07	1.7609E+02
6	2,637	3.895E-03	2.8648015E-01	2.485423E-06	6.92E-07	3.83E-07	2.8278E+02
7	3,625	3.322E-03	2.8647983E-01	2.275731E-06	3.81E-07	1.73E-07	4.3195E+02
8	4,906	2.855E-03	2.8647965E-01	2.180707E-06	1.97E-07	7.84E-08	6.6397E+02
9	6,687	2.446E-03	2.8647956E-01	2.137702E-06	1.03E-07	3.54E-08	1.0089E+03
10	9,207	2.084E-03	2.8647951E-01	2.118134E-06	5.42E-08	1.58E-08	1.6366E+03

IV.A.3. Viscous Case Results

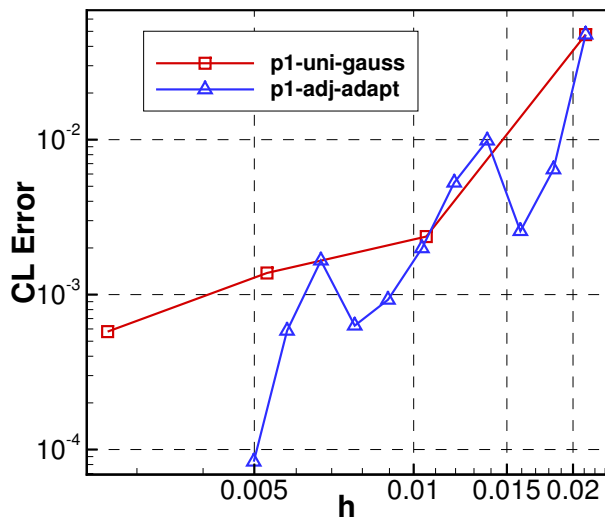
Below figures and tables show the requested results for the viscous flow over a NACA0012 airfoil. Anisotropic adaptations are driven by the output-based error indicator. The optimal refinement option for each element is obtained by the local output error sampling procedures. Uniform h-refinement is performed to compare those adaptation strategies. The CPR method with the Gauss points as the SPs/FPs and the LP approach is used in the discretization. All adaptations start from the refl quadrilateral mesh provided by the workshop website, which has 560  $p_4$  quadrilateral elements.



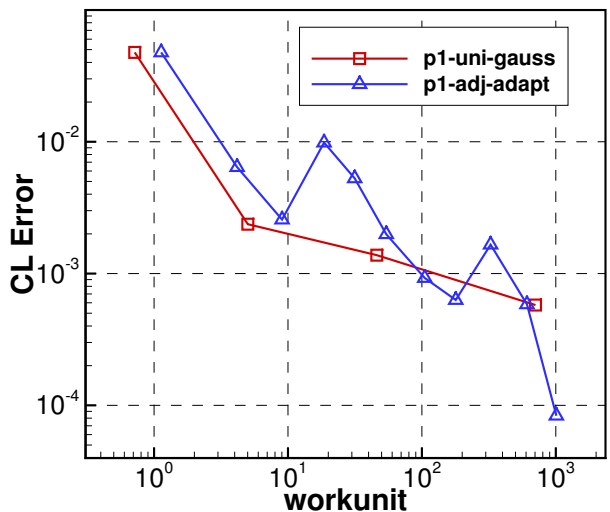
(a)  $C_D$  error vs the length scales



(b)  $C_D$  error vs the work units

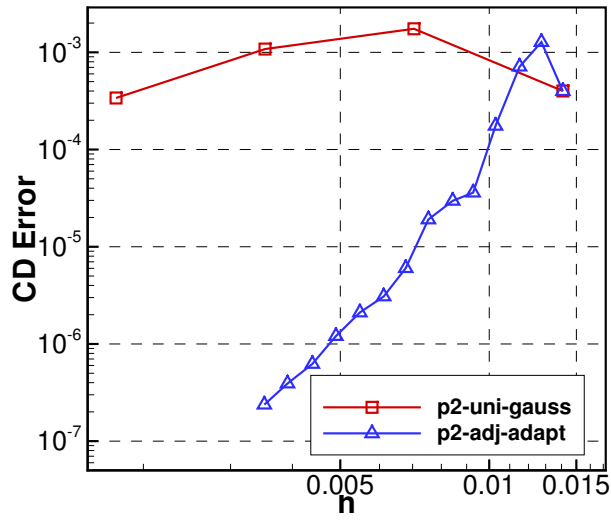


(c)  $C_L$  error vs the length scales

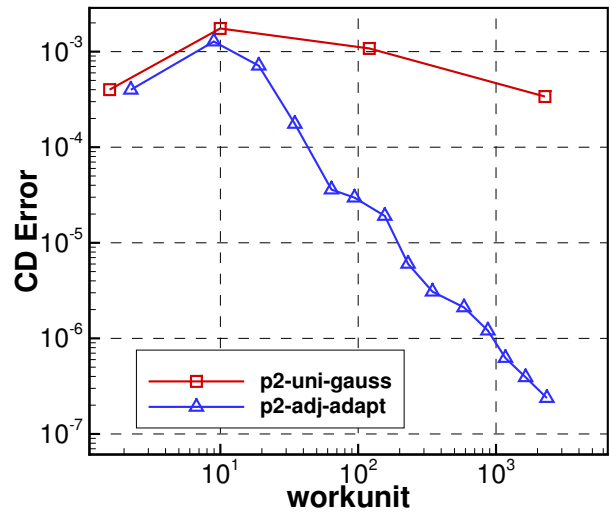


(d)  $C_L$  error vs the work units

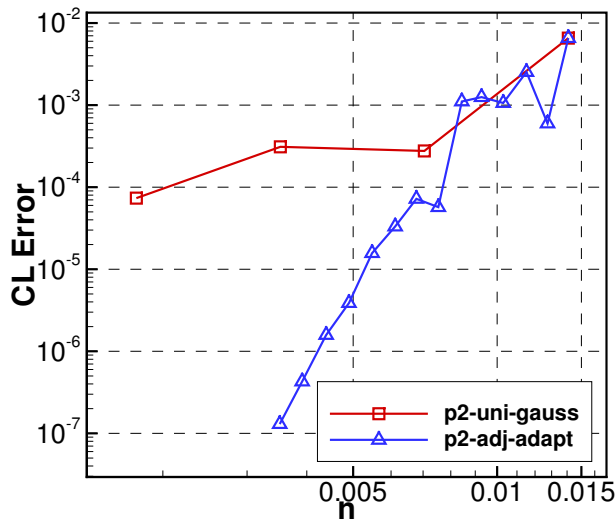
Figure IV.11: NACA 0012 airfoil at  $M_0 = 0.5$ ,  $\alpha = 1^\circ$ ,  $Re = 5000$  ( $p = 1$ ).



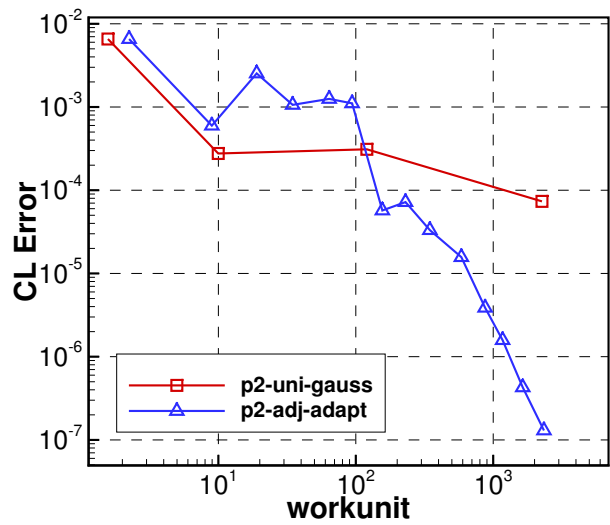
(a)  $C_D$  error vs the length scales



(b)  $C_D$  error vs the work units

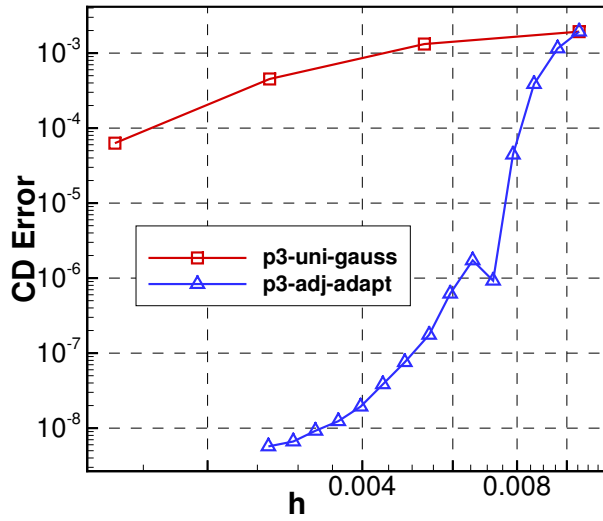


(c)  $C_L$  error vs the length scales

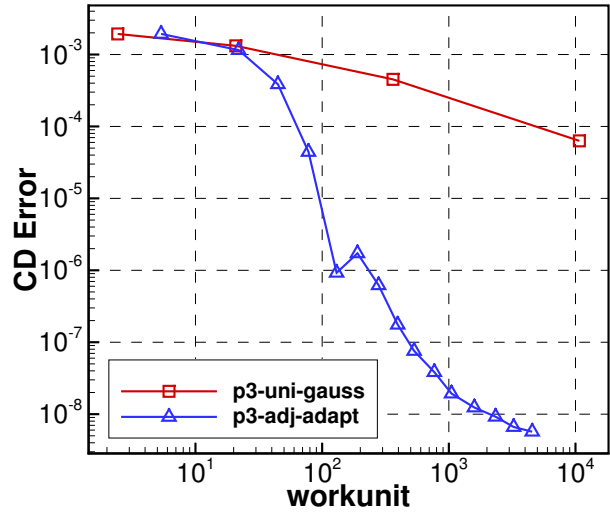


(d)  $C_L$  error vs the work units

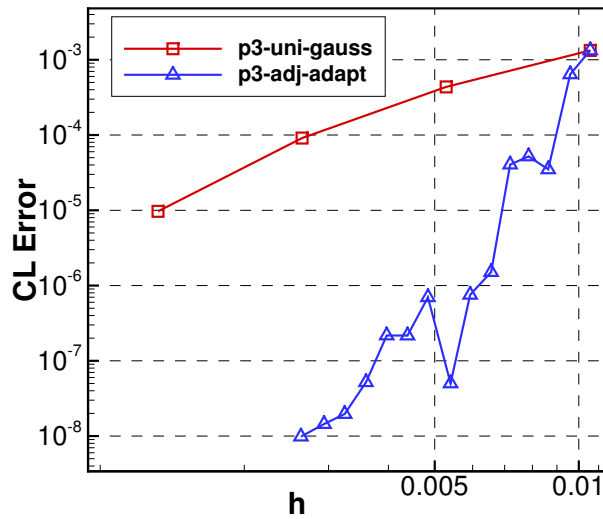
Figure IV.12: NACA 0012 airfoil at  $M_0 = 0.5$ ,  $\alpha = 1^\circ$ ,  $Re = 5000$  ( $p = 2$ ).



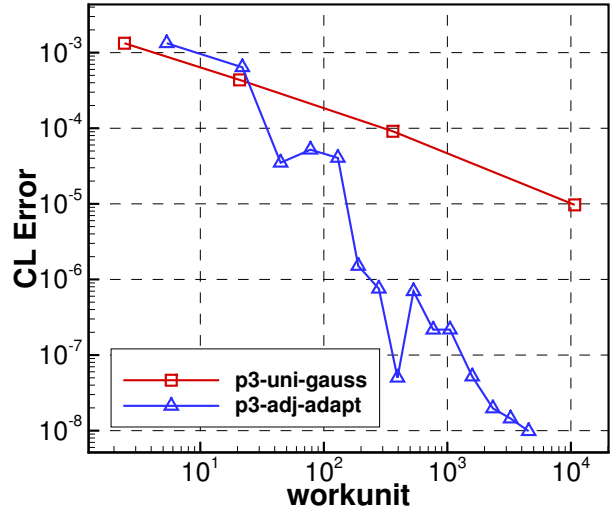
(a)  $C_D$  error vs the length scales



(b)  $C_D$  error vs the work units

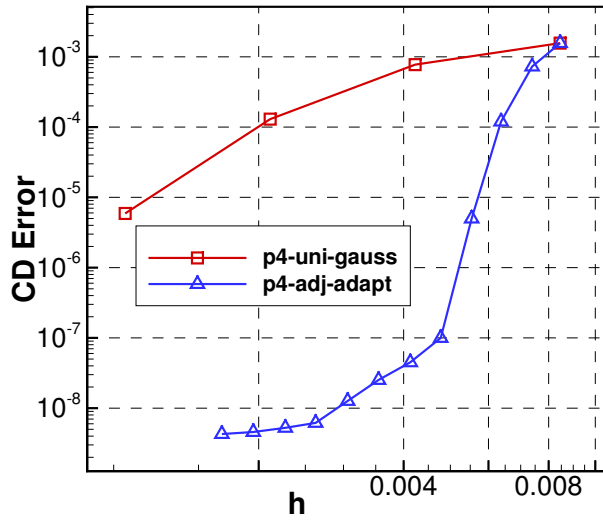


(c)  $C_L$  error vs the length scales

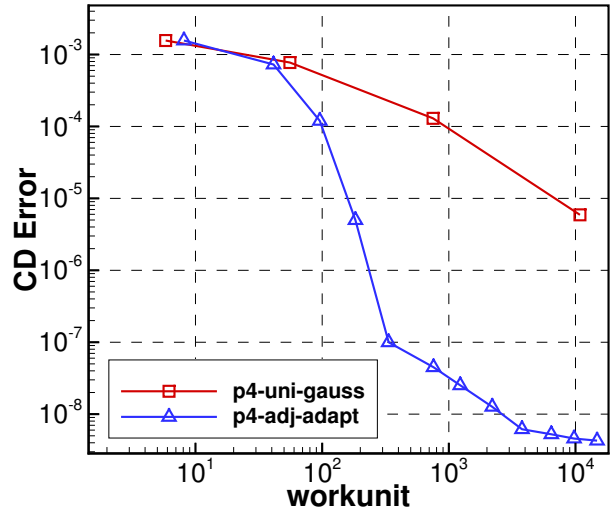


(d)  $C_L$  error vs the work units

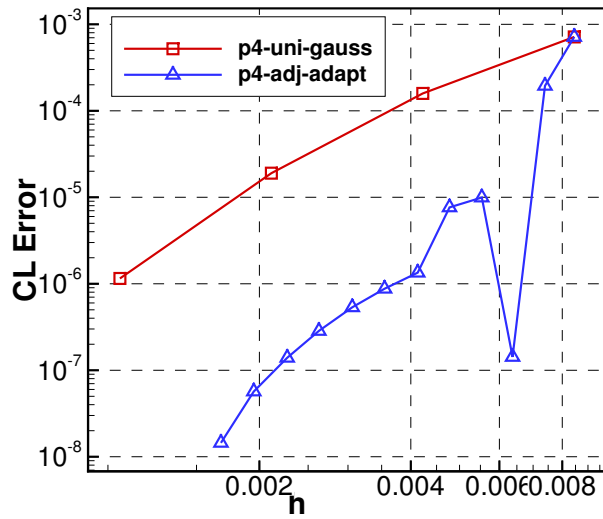
Figure IV.13: NACA 0012 airfoil at  $M_0 = 0.5$ ,  $\alpha = 1^\circ$ ,  $Re = 5000$  ( $p = 3$ ).



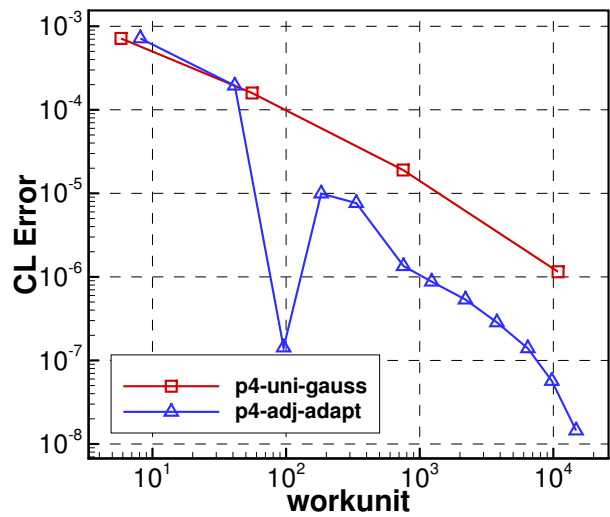
(a)  $C_D$  error vs the length scales



(b)  $C_D$  error vs the work units



(c)  $C_L$  error vs the length scales



(d)  $C_L$  error vs the work units

Figure IV.14: NACA 0012 airfoil at  $M_0 = 0.5$ ,  $\alpha = 1^\circ$ ,  $Re = 5000$  ( $p = 4$ ).



Table 5: NACA 0012 airfoil at  $M_0 = 0.5$ ,  $\alpha = 1^\circ$ ,  $Re = 5000$  ( $p = 1$ ).

adaptation stages	cell	h	$C_L$	$C_D$	$C_L$ error	$C_D$ error	work units
1	560	2.113E-02	6.590882E-02	7.169859E-02	4.76E-02	1.64E-02	1.13E+00
2	741	1.837E-02	1.185211E-02	5.865338E-02	6.42E-03	3.34E-03	4.17E+00
3	988	1.591E-02	2.084095E-02	5.638402E-02	2.57E-03	1.07E-03	9.03E+00
4	1,319	1.377E-02	2.812552E-02	5.614252E-02	9.85E-03	8.26E-04	1.86E+01
5	1,757	1.193E-02	2.354719E-02	5.603645E-02	5.27E-03	7.20E-04	3.15E+01
6	2,327	1.037E-02	2.026147E-02	5.583968E-02	1.99E-03	5.23E-04	5.42E+01
7	3,127	8.941E-03	1.919902E-02	5.560721E-02	9.26E-04	2.90E-04	1.05E+02
8	4,175	7.738E-03	1.890365E-02	5.551471E-02	6.30E-04	1.98E-04	1.79E+02
9	5,605	6.679E-03	1.993018E-02	5.545620E-02	1.66E-03	1.39E-04	3.26E+02

Table 6: NACA 0012 airfoil at  $M_0 = 0.5$ ,  $\alpha = 1^\circ$ ,  $Re = 5000$  ( $p = 2$ ).

adaptation stages	cell	h	$C_L$	$C_D$	$C_L$ error	$C_D$ error	work units
1	560	1.409E-02	1.171683E-02	5.571586E-02	6.56E-03	3.99E-04	2.24E+00
2	684	1.275E-02	1.767606E-02	5.404131E-02	5.97E-04	1.28E-03	8.96E+00
3	838	1.151E-02	1.574251E-02	5.460473E-02	2.53E-03	7.12E-04	1.90E+01
4	1,048	1.030E-02	1.721234E-02	5.514154E-02	1.06E-03	1.75E-04	3.47E+01
5	1,291	9.277E-03	1.702174E-02	5.535293E-02	1.25E-03	3.60E-05	6.40E+01
6	1,561	8.437E-03	1.716663E-02	5.534657E-02	1.11E-03	2.97E-05	9.40E+01
7	1,958	7.533E-03	1.821626E-02	5.533599E-02	5.71E-05	1.91E-05	1.56E+02
8	2,418	6.779E-03	1.820133E-02	5.532291E-02	7.21E-05	6.02E-06	2.30E+02
9	2,967	6.120E-03	1.824021E-02	5.531997E-02	3.32E-05	3.08E-06	3.46E+02
10	3,704	5.477E-03	1.825766E-02	5.531900E-02	1.57E-05	2.11E-06	5.86E+02
11	4,628	4.900E-03	1.827725E-02	5.531810E-02	3.87E-06	1.21E-06	8.73E+02
12	5,764	4.391E-03	1.827180E-02	5.531751E-02	1.58E-06	6.23E-07	1.17E+03
13	7,264	3.911E-03	1.827295E-02	5.531728E-02	4.28E-07	3.92E-07	1.64E+03
14	9,014	3.511E-03	1.827351E-02	5.531713E-02	1.30E-07	2.38E-07	2.34E+03

Table 7: NACA 0012 airfoil at  $M_0 = 0.5$ ,  $\alpha = 1^\circ$ ,  $Re = 5000$  ( $p = 3$ ).

adaptation stages	cell	h	$C_L$	$C_D$	$C_L$ error	$C_D$ error	work units
1	560	1.056E-02	1.9604671E-02	5.3382131E-02	1.33E-03	1.93E-03	5.35E+00
2	679	9.594E-03	1.8913361E-02	5.4164170E-02	6.40E-04	1.15E-03	2.19E+01
3	839	8.631E-03	1.8308373E-02	5.4930589E-02	3.50E-05	3.86E-04	4.47E+01
4	1,013	7.855E-03	1.8221372E-02	5.5272616E-02	5.20E-05	4.43E-05	7.80E+01
5	1,210	7.187E-03	1.8232878E-02	5.5317813E-02	4.05E-05	9.23E-07	1.30E+02
6	1,453	6.559E-03	1.8274889E-02	5.5318613E-02	1.51E-06	1.72E-06	1.90E+02
7	1,778	5.929E-03	1.8272625E-02	5.5317510E-02	7.54E-07	6.20E-07	2.79E+02
8	2,147	5.395E-03	1.8273329E-02	5.5317065E-02	5.01E-08	1.75E-07	3.95E+02
9	2,669	4.839E-03	1.8274078E-02	5.5316966E-02	6.99E-07	7.57E-08	5.32E+02
10	3,249	4.386E-03	1.8273596E-02	5.5316928E-02	2.17E-07	3.84E-08	7.68E+02
11	3,968	3.969E-03	1.8273596E-02	5.5316909E-02	2.17E-07	1.93E-08	1.05E+03
12	4,844	3.592E-03	1.8273431E-02	5.5316902E-02	5.20E-08	1.24E-08	1.59E+03
13	5,946	3.242E-03	1.8273399E-02	5.5316899E-02	1.97E-08	9.21E-09	2.34E+03
14	7,253	2.935E-03	1.8273393E-02	5.5316897E-02	1.44E-08	6.63E-09	3.25E+03
15	9,060	2.626E-03	1.8273369E-02	5.5316896E-02	9.84E-09	5.70E-09	4.55E+03

Table 8: NACA 0012 airfoil at  $M_0 = 0.5$ ,  $\alpha = 1^\circ$ ,  $Re = 5000$  ( $p = 4$ ).

adaptation stages	cell	h	$C_L$	$C_D$	$C_L$ error	$C_D$ error	work units
1	560	8.452E-03	1.8988753E-02	5.3751893E-02	7.15E-04	1.56E-03	8.11E+00
2	732	7.392E-03	1.8468071E-02	5.4590469E-02	1.95E-04	7.26E-04	4.13E+01
3	985	6.373E-03	1.8273236E-02	5.5197245E-02	1.43E-07	1.20E-04	9.58E+01
4	1,305	5.536E-03	1.8283319E-02	5.5311905E-02	9.94E-06	4.98E-06	1.83E+02
5	1,754	4.775E-03	1.8281023E-02	5.5316990E-02	7.64E-06	9.98E-08	3.35E+02
6	2,347	4.128E-03	1.8274724E-02	5.5316935E-02	1.34E-06	4.49E-08	7.57E+02
7	3,178	3.548E-03	1.8274256E-02	5.5316915E-02	8.77E-07	2.52E-08	1.23E+03
8	4,272	3.060E-03	1.8273914E-02	5.5316903E-02	5.35E-07	1.27E-08	2.20E+03
9	5,799	2.626E-03	1.8273664E-02	5.5316896E-02	2.85E-07	6.17E-09	3.78E+03
10	7,750	2.272E-03	1.8273518E-02	5.5316895E-02	1.39E-07	5.25E-09	6.44E+03
11	10,525	1.949E-03	1.8273436E-02	5.5316895E-02	5.68E-08	4.58E-09	9.74E+03
12	14,215	1.677E-03	1.8273393E-02	5.5316894E-02	1.45E-08	4.28E-09	1.48E+04